Adsorption Microcalorimetry: Recent Advances in Instrumentation and Application

Matthew C. Crowe[1] and Charles T. Campbell[2]

[1]Analytical Sciences, The Dow Chemical Company, Spring House, Pennsylvania 19477; email: crowe@dow.com

[2]Department of Chemistry, University of Washington, Seattle, Washington 98195-1700; email: campbell@chem.washington.edu

Annu. Rev. Anal. Chem. 2011. 4:41–58

First published online as a Review in Advance on March 1, 2011

The *Annual Review of Analytical Chemistry* is online at anchem.annualreviews.org

This article's doi: 10.1146/annurev-anchem-061010-113841

1936-1327/11/0719-0041$20.00

Keywords

calorimetry, surface reactions, nanoparticle sintering, catalysis, photovoltaics

Abstract

Adsorption microcalorimetry measures the energetics of adsorbate-surface interactions and can be performed by use of several different techniques. This review focuses on three methods: single-crystal adsorption calorimetry (SCAC), isothermal titration calorimetry (ITC), and electrochemical adsorption calorimetry. SCAC is a uniquely powerful technique that has been applied to a variety of atoms and molecules that represent a large variety of well-defined adsorbate species on a wide range of single-crystal surfaces. ITC and electrochemical microcalorimetry are useful for studying adsorption energies in liquid solutions (on surfaces of suspended powders) and at the electrode-electrolyte interface, respectively. Knowledge of the energetics of adsorbate formation is valuable to ongoing research in many fields, including catalysis, fuel cells, and solar power. In addition, calorimetric measurements serve as benchmarks for the improvement of computational approaches to understanding surface chemistry. We review instrumentation and applications, emphasizing our own work.

1. INTRODUCTION

UHV: ultrahigh vacuum

SCAC: single-crystal adsorption calorimetry

ITC: isothermal titration calorimetry

AES: Auger electron spectroscopy

XPS: X-ray photoelectron spectroscopy

LEIS: low-energy ion scattering

DFT: density functional theory

Heat is generally evolved or absorbed over the course of a chemical reaction, and calorimetric measurements aim to quantify this heat to provide information about reaction thermodynamics. In adsorption calorimetry, the reactions of interest involve the adsorption of atomic or molecular species onto a surface, and the heat exchanged with the surface can manifest as a temperature change in the substrate and/or the surrounding environment. Adsorption calorimetric measurements take advantage of these measurable changes to provide valuable information about surface reactions of interest. For molecular adsorbates, the reaction measured can be intact adsorption, dissociative adsorption, or even adsorbate-adsorbate coupling. Additionally, because the energy of adsorption often varies strongly with surface coverage, microcalorimetric techniques whose sensitivity is sufficient to measure submonolayer coverages of adsorbates show how coverage affects reaction energies. Three calorimetry techniques used to study adsorption thermodynamics with submonolayer sensitivity are ultrahigh-vacuum (UHV) single-crystal adsorption calorimetry (SCAC), isothermal titration calorimetry (ITC), and electrochemical microcalorimetry.

It is possible to generate valuable information about the energetics of adsorbate-surface interactions with other techniques such as temperature-programmed desorption (TPD) and equilibrium isotherm analysis. However, adsorption energy measurement using these techniques is possible only for cases in which adsorption is reversible. If structural changes occur prior to desorption, all information about the original adsorbate-surface bonding of interest is lost. Such situations are common and include bond breaking or forming in adsorbed molecules or molecular fragments (especially with catalytic intermediates) or, for atomic adsorbates, alloy formation with the substrate or agglomeration into three-dimensional particles. These problems severely limit the applicability of techniques such as TPD and equilibrium isotherm analysis.

SCAC, however, can accurately measure adsorbate-binding strengths in cases of irreversible adsorption because SCAC involves direct measurement of the energy released upon the adsorption of an analyte to a surface. UHV SCAC measures the change in substrate temperature that arises from analyte adsorption. Determining reaction enthalpies per mole of adsorbate from substrate temperature changes requires knowledge of the number of adsorbing species as well as the instrument's response to a known quantity of energy. Therefore, in addition to calorimetry, molecular beam flux, sticking probability, and energy calibration measurements must be performed. Meaningful interpretation of the resulting reaction enthalpies in terms of the number and nature of the bonds being formed and/or broken is most successful when a great deal is known about the structure of the reaction product. Indeed, SCAC has typically been applied to adsorbate-substrate combinations that have been thoroughly characterized. In UHV–surface science studies, such structural information is typically obtained with techniques such as Auger electron spectroscopy (AES), X-ray photoelectron spectroscopy (XPS), surface vibrational spectroscopy, low-energy electron diffraction, low-energy ion scattering (LEIS), and scanning tunneling microscopy (STM). Also, periodic density functional theory (DFT) calculations are often important in aiding data interpretation. This technique provides a productive feedback cycle because the measured reaction energies, in turn, provide direct tests of the energy accuracy of computational methods such as DFT. Indeed, SCAC has been powerful in elucidating some of the shortcomings of periodic DFT for surface reaction energies (1).

SCAC has been developed and applied by several research groups to evaluate surface reactions that are important in catalysis and microelectronics. It has generated valuable data for systems involving molecular adsorption onto single-crystal and size-controlled nanoparticle surfaces as well as metal atom adsorption onto single-crystal metal, oxide, carbide, and semiconductor surfaces. These data have significantly improved our understanding of the surface chemistries that

occur in these systems. Because it provides valuable information that is inaccessible through other techniques, SCAC is very important in any area of research and technology that involves solid surfaces.

The same techniques developed for SCAC can also be applied to solid surfaces that are not single crystals. For example, we discuss an adaptation of these methods to study polymer surfaces, whereby the polymer is spin-coated directly onto the surface of the heat detector (which allows for 10-fold-greater sensitivity in heat detection), and their application to the study of metal-polymer interfaces relevant to photovoltaic device fabrication.

ITC is also used for adsorption calorimetric measurements, and in stark contrast with UHV SCAC instruments, it allows the investigation of adsorption events that take place from a liquid solution onto a solid surface. ITC involves monitoring the heat input necessary to keep a sample cell and a reference cell at the same temperature when a chemical reaction is taking place in the sample cell (2). For applications in adsorption calorimetry, the solid of interest is in the form of a powder, which is suspended in a liquid and placed into the sample cell. The adsorbing species is injected into the same cell as a solute in small, reproducible volumes of solution. The reference cell is filled with the same solution as the sample cell, minus the reacting solute species. Below, we discuss results in which adsorption events that are crucial to a biologically relevant salivary process were investigated with ITC and equilibrium adsorption isotherm measurements, and we give structural information about the adsorbed protein provided by nuclear magnetic resonance (NMR).

Lastly, we describe an exciting recent development in electrochemical adsorption microcalorimetry (3–5). Such measurements use the same heat-detection method utilized by our group for SCAC, but, instead of a pulsed molecular beam of the adsorbing gas, they involve pulse-like adsorption or reaction of liquid-phase solute species on a working electrode surface, initiated by a step change in voltage or a current pulse. Because these measurements are made on a flat surface, they can also be applied to single-crystal surfaces. Voltage-current pulses are a convenient way to initiate a rapid adsorption event from liquid solution, but in principle such an event could be initiated instead by injection of a solution. These results imply that adsorption energies may soon be measured from a liquid solution on single-crystal surfaces even in the absence of electrochemical potential control. The challenge would be to design a flow cell with stringent enough temperature control during rapid solute injection; the design would probably use a reference cell to compensate for some of the temperature difference arising from the injection event.

2. SINGLE-CRYSTAL ADSORPTION CALORIMETRY: HISTORY AND INSTRUMENTATION DEVELOPMENTS

In the early 1990s, Sir David King's research group (6–8) pioneered the development of SCAC with the first UHV instrument capable of measuring heats of adsorption on single-crystal surfaces as a function of coverage with a high level of precision. Such instruments, in their current form, utilize a 200-nm-thick single crystal and a HgCdTe infrared optical pyrometer to measure the rise in blackbody radiation emitted from the sample upon adsorption of gas-phase molecules. The back face of the sample is coated with carbon to enhance emissivity, and this, coupled with the sample's low thermal mass, allows measurement of temperature changes on the order of ~0.1 K. Unfortunately, due to the strong dependency of blackbody radiation efficiency on temperature (signal $\propto T^3$, where T is the sample temperature) (7), this method is limited to the study of reactions that take place at or above ambient temperatures.

In addition to developing an SCAC instrument based on remote infrared detection, King's group (9) tested a pyroelectric detection scheme utilizing a $LiTaO_3$ crystal permanently affixed

PVDF: polyvinylidene fluoride

to the back of a single-crystal sample. This pyroelectric detector allows accurate measurement of adsorption energies as a function of coverage at or below room temperature, but permanently affixing the sample to the $LiTaO_3$ restricts the sample temperature such that effective ordering of the single-crystal surface via annealing is not possible with most materials. The high thermal mass of the detector/sample assembly also results in long sample-temperature equilibration times, which ultimately limits the cleanliness of the sample surface because experiments cannot be performed immediately following sample-surface cleaning (10).

Improving on the pyroelectric detector tested by King's group, Campbell's research group (11–14) developed an SCAC instrument that utilizes a removable pyroelectric heat detector, which (*a*) takes advantage of the detector's ability to perform sensitive calorimetry experiments at or below room temperature and (*b*) allows sample preparation at the necessary high temperatures. This detector setup utilizes a 4-mm-wide, 50-mm-long, 9-μm-thick, uniaxially oriented β–polyvinylidene fluoride (β-PVDF) pyroelectric ribbon, coated on both sides with a thin layer of aluminum. The ribbon is bent into an arc that is pressed into good thermal contact with the back face of a single-crystal sample during calorimetric measurements (but removed between measurements so the sample can be annealed), thereby allowing precise measurement of sample temperature changes as small as a few millikelvins. The PVDF-based detector also increases the sensitivity of SCAC measurements to the point that considerably thicker (up to 75 μm) single-crystal samples can be used, greatly increasing the number of materials available for investigation with adsorption microcalorimetry (12, 15).

Recent improvements to the Campbell group's pyroelectric detector design further extend the types of samples, the energy and temperature ranges, and the reaction intermediates that can be studied with SCAC (16). A recent iteration of this calorimeter design is shown in **Figure 1*a***.

Two significant improvements have been made to this ribbon design since the photograph in **Figure 1*a*** was taken. The first was to remove all the aluminum coating that is not required for the sample ΔT measurement. The aluminum coating on the front and back faces of the PVDF ribbon functions as two electrodes, each of which is characterized by an extent of charging that mirrors the permanent dipole of the pyroelectric material. When this dipole changes due to a temperature change and the electrodes are electrically connected, current flows so that charge on the front- and back-face electrodes eventually reflect the new dipole of the pyroelectric material (17). In the Campbell group's pyroelectric detector, this charge flows through an electrical circuit containing the 10-GΩ resistor (**Figure 1*c***), across which a transient voltage corresponding to a sample-temperature change is measured (16). The only areas of the aluminum coating necessary for calorimetry are those that (*a*) coat the front and back faces of the $4 \times 4\ mm^2$ region of the ribbon in contact with the sample and (*b*) electrically connect these areas to the copper blocks wired to the detector circuit (**Figure 1*c***). Removing unnecessary portions gave markedly improved signal-to-noise (S/N) characteristics (16). The etched-ribbon design is shown in **Figure 1*c***.

The second major improvement to the calorimeter design was to decrease the diameter of the pyroelectric ribbon arc from 6 mm to 3 mm. Doing so allowed sample-temperature changes to be measured more effectively (at least for Pt, which is strong enough to stand the increased ribbon pressure), resulting in a further increased S/N ratio (16).

Together, these improvements to the calorimeter design resulted in a 40-fold increase in sensitivity at 100 K and a pulse-to-pulse standard deviation of 1.3 kJ mol^{-1} for molecular beam pulses containing ~1% of a monolayer (ML). For a 1-μm-thick Pt crystal, this standard deviation corresponds to a temperature change of only 0.15 mK. The detector-to-sample thermal contact and the S/N ratio of this calorimeter can be increased even further through the use of a twin-ribbon detector, in which two pyroelectric ribbons (each with a 1-mm arc) are mounted side by side, but such a setup requires stronger samples (16).

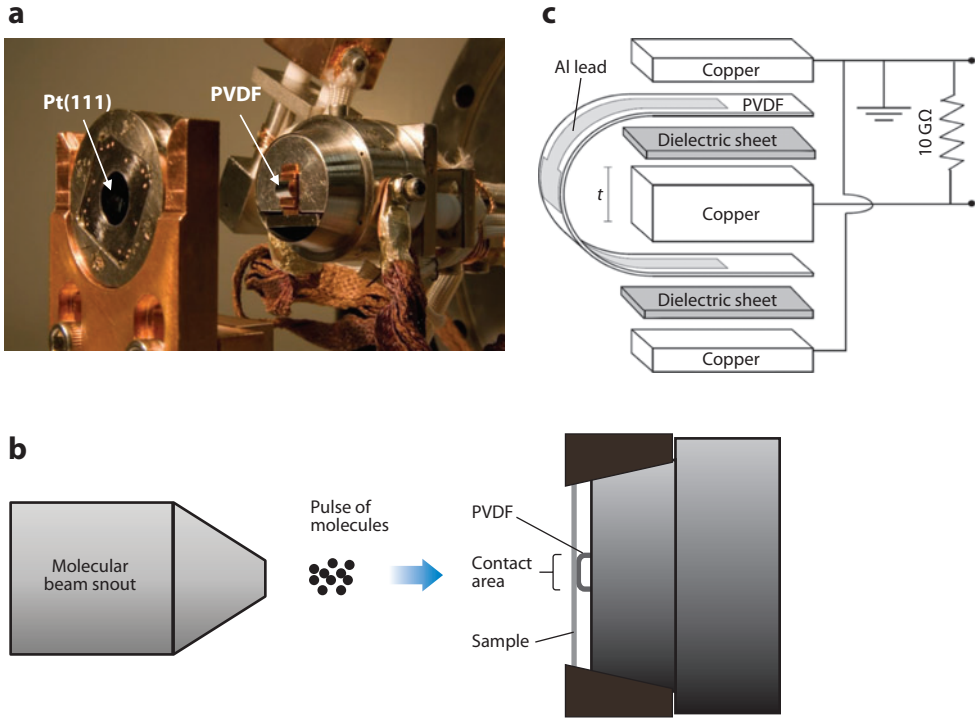

Figure 1

(*a*) The Campbell group's single-crystal adsorption calorimetry (SCAC) pyroelectric heat detector assembly, which houses a polyvinylidene fluoride (PVDF) ribbon (4 mm wide, held in a 6-mm-diameter arc), shown retracted from a single-crystal sample holder that exposes an 8-mm-diameter area of the Pt(111) sample's surface. A linear translator is used to press the pyroelectric detector into good thermal contact with the back face of the sample during heat measurement. The ribbon is fully coated on the front and back faces with a thin layer of aluminum, as received from the manufacturer (Goodfellow). (*b*) Schematic of an SCAC experiment. The molecular beam emits spatiotemporally resolved pulses of gas-phase atoms or molecules that impinge on the sample surface; the pyroelectric heat detector, shown pressed into contact with the back face of a single-crystal sample, measures temperature changes associated with adsorption events. (*c*) Exploded view of the detector assembly, showing the PVDF ribbon with patterned aluminum electrodes, ribbon-mounting hardware, and a portion of the associated electronic circuitry. Sample in panel *a* supplied by Jacques Chevallier (Aarhus University, Denmark). Reprinted with permission from Reference 16. Copyright 2010, American Institute of Physics.

This increased sensitivity has led to two important results. First, the ability to measure very small temperature changes allows the investigation of thicker single crystals, which—particularly when using the twin-ribbon detector—broadens the range of samples that can be studied to include any material that can be mechanically thinned to ~100 μm. Second, through the use of the improved single-ribbon detector system, the limits of detection (3.9 kJ mol^{-1}) and quantitation (13 kJ mol^{-1}) have been decreased to levels that allow the investigation of weak chemisorption and even physisorption interactions between adsorbates and the surface, as has been demonstrated in studies of the adsorption of water onto clean and oxygen-predosed Pt(111) surfaces (W. Lew, M.C. Crowe, E. Karp & C.T. Campbell, manuscript submitted).

Previous measurements by the Wheeler (18), King (9), and Campbell (19) groups involved adsorption calorimetry performed at subambient temperatures. However, in these studies the

temperature of the sample was controlled through the use of a single low-temperature bath. Recently, the Campbell group developed a system in which two streams of dry N_2 gas are flowed through two separate constant-temperature baths. Through variation of the relative flow rates of the two $N_{2(g)}$ streams, the temperature of the calorimeter can be set anywhere between 77 K and 350 K (16, 20), thereby allowing investigation of catalytic intermediates that form at any temperature in this range.

Recently, Punckt et al. (21) developed a technique for detecting temperature changes in single-crystal samples, with the goal of improving heat detection in SCAC. In this method, the deformation of a thin single-crystal sample resulting from thermoelastic stress is measured with a Michelson interferometer–based instrument, in which the sample functions as one of the mirrors in the interferometer. The first experiments that used this system were performed without energy calibration, and thus only qualitative analysis of the results was possible. Nonetheless, this technique can measure heat released due to catalytic reactions, such as CO oxidation, on the Pt(110) surface as a function of time. Particularly impressive are the spatiotemporal patterns of catalyst surface temperature recorded using this technique, in which the extent of local deformation (due to surface expansion) is proportional to the temperature change (heat release). These data allowed the authors to relate observations such as the rate of reaction front propagation to specific experimental conditions, such as O_2 partial pressure and catalyst temperature. To make the instrument capable of quantitative adsorption microcalorimetry experiments, with figures of merit theoretically very competitive with those of the King and Campbell groups' calorimeters, Punckt et al. (21) proposed a design that involves laser irradiation of the sample for energy calibration as well as quantitative ellipsometry to determine adsorbate coverage.

The applications of SCAC to determine the heats of adsorption of molecules onto single-crystal metal surfaces have been reviewed elsewhere (1, 10, 22). This research has elucidated the heats of formation of adsorbed molecules and molecular fragments that are known intermediates in catalytic and electrocatalytic reactions and, thus, has provided important new insights into the potential-energy diagrams for catalytic reaction mechanisms.

3. UNDERSTANDING THE FUNDAMENTAL THERMODYNAMICS OF SINTERING OF SUPPORTED METAL NANOPARTICLE CATALYSTS

Transition-metal nanoparticles dispersed across the surfaces of oxide and carbon support materials form the basis for most solid catalysts used for industrial chemical reactions that produce fuels and clean up pollution associated with the generation and use of fuels. They also serve as the best electrocatalysts for fuel cells and photocatalysts for harvesting solar energy. Sintering (i.e., agglomeration or ripening into fewer, larger particles) is one of the main modes for deactivation of such catalysts. SCAC of metal adsorption can be used to measure the energetic stability of metal atoms in nanoparticles supported on well-defined oxide surfaces (23–31), which is improving our understanding of the different sintering rates of catalyst materials (32–34).

Recent studies compared the energetics of Ag atoms adsorbing onto Ag nanoparticles during their growth on MgO(100) and reduced CeO_2(111) surfaces. The results provide great insight into why metal nanoparticles demonstrate greater sinter resistance on CeO_2 than on other support materials (34). Specifically, the adsorption energies of Ag atoms onto MgO(100) and three slightly reduced CeO_2(111) thin film surfaces were measured as a function of Ag coverage. Nanoparticle diameter was determined as a function of Ag coverage using surface-analysis techniques (AES and LEIS), nanoparticle growth models, and the density of bulk Ag (5.9×10^{22} atoms cm^{-3}). Together, these observations allowed the authors (34) to determine the energetics of Ag atom adsorption to the nanoparticle surface as a function of nanoparticle

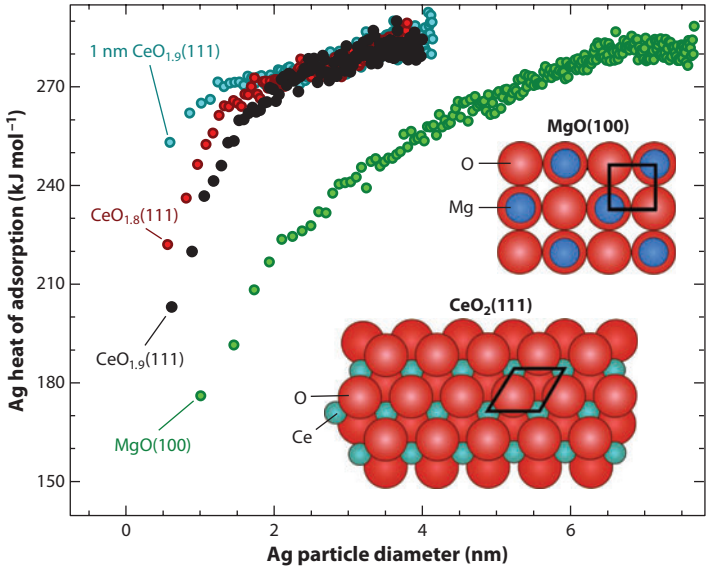

Figure 2

Measured heat of Ag atom adsorption on oxide surfaces, versus the diameter of the Ag particle to which it adsorbs, for four different surfaces: two 4-nm-thick CeO_2(111) films with different extents of surface reduction (CeO_{2-x}, $x = 0.1$ and 0.2), a 1-nm-thick $CeO_{1.9}$(111) film, and a 4-nm-thick MgO(100) film. The first three films were grown on Pt(111), and the fourth was grown on Mo(100). (*Right*) Structural models for perfect CeO_2(111) and MgO(100); black lines indicate their unit cells. From Reference 34. Reprinted with permission from the American Association for the Advancement of Science.

diameter (**Figure 2**). These data show that, for a given nanoparticle size, Ag atoms release more energy upon adsorption to nanoparticles supported on reduced ceria surfaces compared with MgO(100). Also, for all surfaces studied, as more Ag atoms adsorb, the adsorption energies approach the heat of adsorption of Ag on bulk Ag: 285 kJ mol^{-1}. Perhaps the most significant result (**Figure 2**) is that Ag atoms adsorb with energies similar to that observed for bulk Ag for much smaller nanoparticles on reduced ceria (2–4 nm) than on MgO(100) (6 nm). This means that, for Ag atoms in ceria-supported Ag nanoparticles as small as 1.5–2 nm, there is very little thermodynamic driving force to sinter into larger particles, given that Ag atoms in bulk Ag are only 10–15 kJ mol^{-1} more stable. In contrast, on MgO(100), an Ag atom in a 2-nm particle is ~65 kJ mol^{-1} less stable than in bulk Ag; therefore, there is a significant driving force toward the formation of larger particles. The data in **Figure 2** also show that Ag atoms adsorb with higher energies on 4-nm-thick $CeO_{1.8}$(111) and 1-nm-thick $CeO_{1.9}$(111) films than on 4-nm-thick $CeO_{1.9}$(111). This finding indicates that the creation of more oxygen vacancies in a ceria support or utilizing a thinner support layer even further stabilizes Ag nanoparticles, particularly for nanoparticle diameters less than 1.5 nm.

Farmer & Campbell (34) integrated these heats versus coverage to determine the adhesion energy of Ag nanoparticles to the support material; they found that it is much greater on the ceria surfaces than on MgO(100). Interestingly, the measured adhesion energies for 3.6-nm-diameter ceria-supported Ag nanoparticles were very similar to the Ag-Ag adhesion energy in bulk Ag. To explain why Ag atoms form nanoparticles, as opposed to simply wetting a surface characterized by such strong surface-adatom binding, the authors point out that the Ag nanoparticles probably adsorb to regions of the surface with high defect densities (locally). At surface defects (steps, kinks, oxygen vacancies), the local adhesion energy is probably higher than on stoichiometric

CeO_2(111) terraces, and so the measured adhesion energies may reflect the energies associated with Ag adsorbing to these defect regions, anchoring the nanoparticles in place. In addition, the authors discuss the likelihood of stress at the lattice-mismatched Ag-ceria interface, which would grow with Ag particle size and both limit the size and create effective particle-particle repulsions that inhibit sintering. Although sinter resistance of metal nanoparticles supported on ceria surfaces has been reported elsewhere (35–37), these experimental measurements are the first to clarify the fundamental driving forces behind this enhanced sinter resistance.

4. DETERMINING PARTICLE-SIZE DEPENDENCE OF THE ENERGETICS OF ADSORPTION ONTO SUPPORTED CATALYST NANOPARTICLES

Particle size affects the activity of some late transition-metal catalysts. Single-crystal adsorption microcalorimetry experiments performed recently at the Fritz Haber Institute involved measuring the heat of adsorption of CO onto Fe_3O_4(111)-supported Pd nanoparticles of various sizes. Both the construction of the SCAC instrument and the microcalorimetry measurements were collaborative efforts involving researchers from the laboratories of Schauermann, Freund, and Campbell (38). These measurements calorimetrically probed, for the first time, the dependency of adsorption energetics of a catalytically relevant molecule (CO) on well-characterized nanoparticles of various sizes on a single-crystal oxide surface. As mentioned above, SCAC is the technique of choice for these measurements because (*a*) it does not modify the particles during measurement and (*b*) it does not require reversible adsorption (which would occur only at higher temperatures, at which the Pd particles might sinter). To measure adsorption energetics in the absence of adsorbate-adsorbate interactions (which can be attractive or repulsive), measurements were made under conditions of low adsorbate coverage.

In an earlier study by Freund's group (39), a well-defined Fe_3O_4(111) surface was grown on thin Pt(111) crystal, and Pd particles were deposited onto this surface to prepare nanoparticles of specific sizes. STM images (**Figure 3*a–c***) show the controlled particle growth resulting from the deposition of 0.3, 4, and 7 Å Pd, respectively, onto the Fe_3O_4(111) surface (39). The heat of adsorption of CO was then measured on such surfaces (38). This was done at the low-coverage limit to measure heats of adsorption that depend only on the strength of binding of CO to the nanoparticle surface. The results of these measurements are shown in **Figure 3*d***. As nanoparticles decrease in size, the number of defect sites (steps, kinks, corners) relative to terrace sites increases. Because adsorption onto low–coordination defect sites is typically more exothermic than adsorption onto comparable terrace sites, one might expect that, with decreasing nanoparticle size, the heat of adsorption of the molecules would increase. Interestingly, the heat of adsorption of CO onto Pd nanoparticles decreased with decreasing particle size, indicating that the percentage of low-coordination sites is not the dominant variable affecting molecular adsorption energetics in this system.

These pioneering studies foreshadow that SCAC measurements will provide important insight into the still poorly understood effects of metal-particle size and support on catalytic activity. These are the two main structural parameters used to tune metal catalyst performance.

5. STUDYING THE FORMATION OF THE METAL-POLYMER INTERFACE WITH ULTRAHIGH-VACUUM ADSORPTION MICROCALORIMETRY

As mentioned above, the same pyroelectric heat detector material used for SCAC in our lab can be applied to adsorption microcalorimetry of adsorption events that occur on spin-coated polymer surfaces. Although these surfaces are not as well defined or extensively characterized as

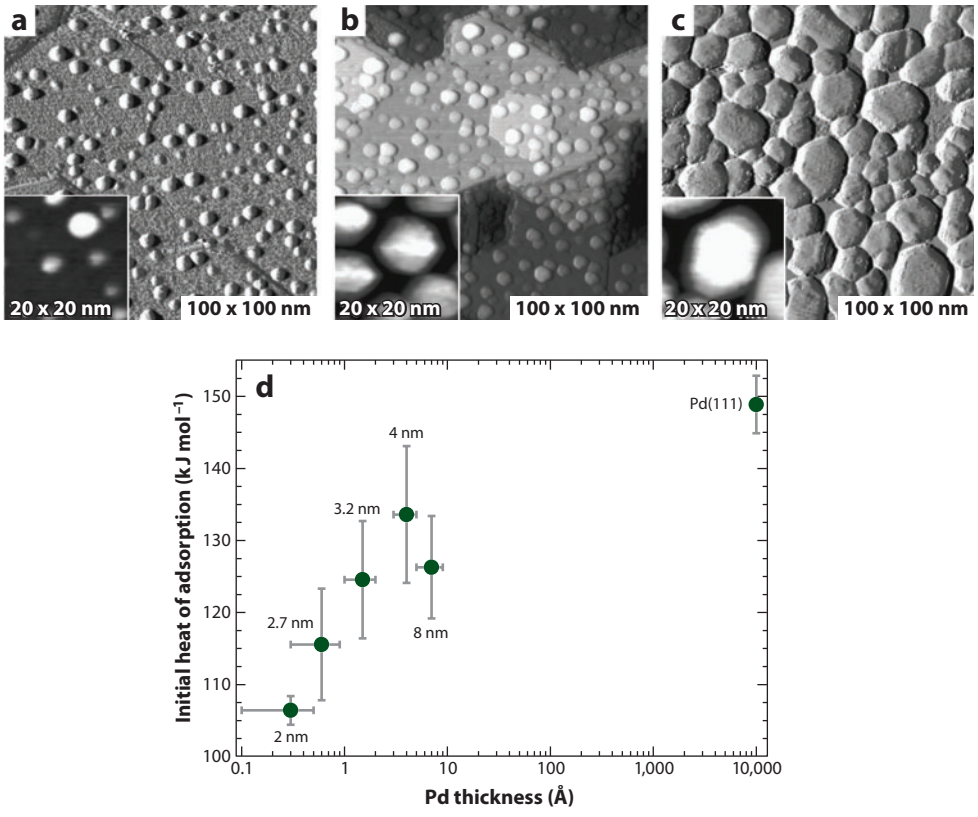

Figure 3

Scanning tunneling microscopy images of Pd on Fe_3O_4(111) after preparation and annealing at 600 K for nominal Pd coverages of (*a*) 0.3 Å, (*b*) 4 Å, and (*c*) 7 Å, which correspond to Pd nanoparticles measuring 2 nm, 4 nm, and 8 nm in diameter, respectively. (*d*) The initial heat of CO adsorption plotted as a function of Pd-deposition thickness (nanoparticle sizes are indicated). The error bars represent the standard deviation of the four to six experimental data sets used to generate each point. Adapted from Reference 38.

single crystals, measuring the heats of surface reactions can provide valuable information, particularly when the measurements are coupled with other surface-analysis techniques and theoretical calculations. A good example of this is the recent work by Zhu et al. (40) and Bebensee et al. (41) characterizing the formation of the Ca–poly(3-hexylthiophene) (P3HT) interface. These researchers utilized LEIS, XPS, adsorption microcalorimetry, and DFT calculations to characterize the regioregular P3HT (rr-P3HT) surface before and after the adsorption of various coverages of Ca metal. Adsorption microcalorimetry was used to directly measure the energetics of the interface formation, whereas XPS, LEIS, and DFT helped explain which chemical reactions correspond to the measured energies. The interface between Ca and rr-P3HT is interesting because these materials form one of the best-performing electrode-polymer combinations for photovoltaic (solar cell) applications (42–46). P3HT chains arranged in a regioregular orientation are shown in **Figure 4*a***. **Figure 4*b*** depicts the sample assembly used for adsorption calorimetry.

For all the surface analyses, Ca metal was vapor-deposited onto an rr-P3HT film that had been outgased under vacuum to remove volatile contaminants. This method is very similar to that typically employed in the preparation of electrode-polymer contacts in organic electronic devices

P3HT: poly(3-hexylthiophene)

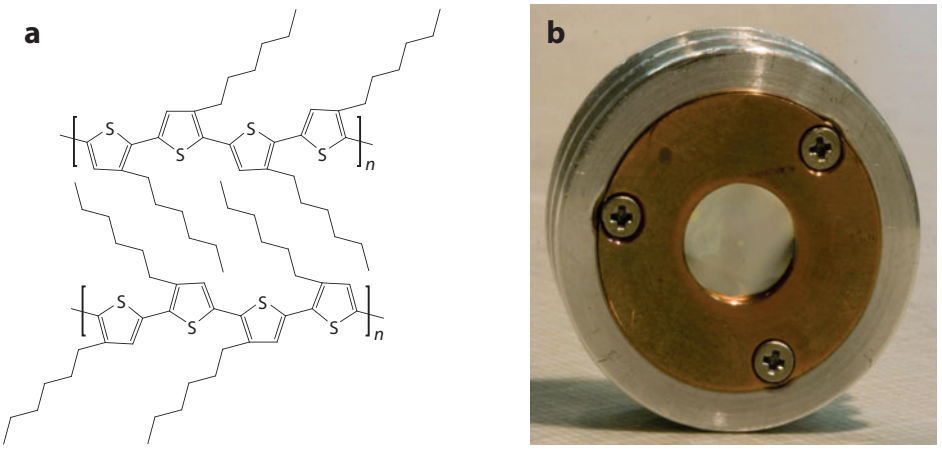

Figure 4

(*a*) Molecular structures depicting regioregular orientation of adjacent poly(3-hexylthiophene) (P3HT) chains (62). (*b*) Sample platen holding a β–polyvinylidene fluoride foil that has been spin-coated with regioregular P3HT, producing a bulk-like polymer thin film suitable for calorimetric, sticking probability, and low-energy ion scattering measurements. Adapted from Reference 63.

(40). The results of LEIS experiments show that the Ca film does not grow in a layer-by-layer fashion, but instead adsorbs as thick three-dimensional islands and/or diffuses below the polymer surface. XPS of the P3HT surface following deposition of different amounts of Ca shows that, whereas the C 1s electron-binding energies remain approximately the same (apart from a slight shift to higher binding energy due to band bending), S 2p signals indicate the formation of sulfur species with electrons of much lower binding energy than observed with the pristine polymer (0 ML Ca coverage; 1 ML $= 7.4 \times 10^{14}$ Ca atoms cm^{-2}) after the deposition of as little as 0.5 ML Ca (**Figure 5*a***) (40). At lower X-ray energy, at which XPS is more surface sensitive, this reaction is already obvious at 0.05 ML Ca (40). The appearance of these peaks indicates that Ca reacts strongly with the sulfur atoms in P3HT polymer films.

The adsorption calorimetry data shown in **Figure 5*b*** substantiate the hypothesis that an energetic reaction takes place upon Ca adsorption to the P3HT surface with an initial reaction enthalpy of 405 kJ mol^{-1} of adsorbed Ca. With the exception of some initial data points that indicate reaction enthalpies of up to 600 kJ mol^{-1}—which probably correspond to the reaction of Ca with impurities below the detection limit of AES and XPS—these calorimetry data show that, as Ca is deposited onto the polymer surface, the reaction enthalpy reaches 405 kJ mol^{-1} from 0 to ~0.5 ML of Ca adsorbed, and then decreases gradually until it reaches the heat of sublimation of Ca [ΔH_{sub}(Ca)]. At higher coverages, obtaining a value equal to Ca's enthalpy of sublimation is to be expected, given that the calorimetric measurement is mainly of Ca adsorbing onto Ca islands and, eventually, multilayer Ca.

The combination of XPS and adsorption calorimetry data indicates that an energetic chemical reaction occurs between the adsorbing Ca and the sulfur atom of the polymer's thiophene ring. To formulate a reaction scheme that would explain these data and involve reactants and products with known heats of formation, the following simplified chemical reaction between $Ca_{(g)}$ and $thiophene_{(l)}$ was proposed:

$$\text{thiophene}_{(1)} + \text{Ca}_{(g)} \rightarrow \text{CaS}_{(s)} + \frac{1}{2}\text{cyclooctatetraene}_{(1)}.$$

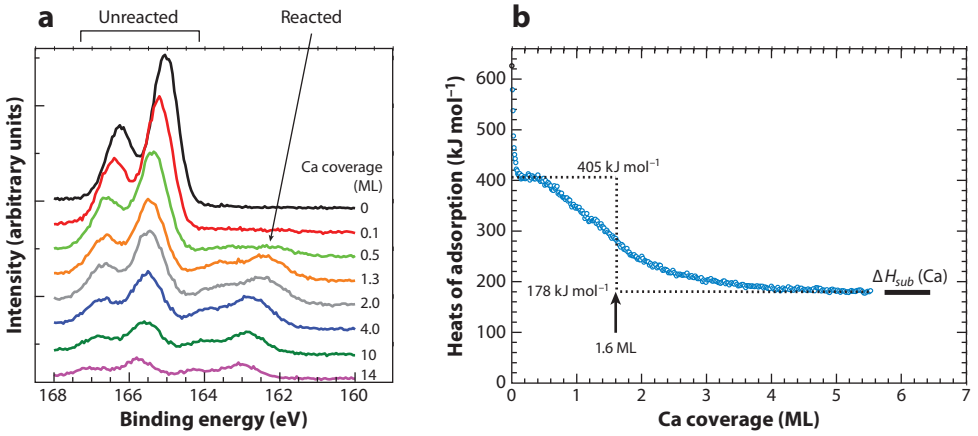

Figure 5

(*a*) Sulfur 2p X-ray photoelectron spectra recorded at a photon energy of 1,487 eV with different coverages of Ca on regioregular poly(3-hexylthiophene) (P3HT) [0–14 monolayers (ML)], showing the appearance of a greatly shifted S 2p peak upon deposition of Ca. (*b*) The differential heat of Ca adsorption to the P3HT surface as a function of Ca coverage, measured at 300 K. These data show a heat of adsorption of ~405 kJ mol^{-1} associated with this reacted S 2p, followed by adsorption heats that gradually decrease toward the heat of sublimation of Ca as coverage increases. The 405 kJ mol^{-1} reaction is attributed to Ca abstracting subsurface thiophene sulfur from P3HT. Reprinted with permission from Reference 40. Copyright 2009, American Chemical Society.

In this reaction, Ca abstracts the sulfur atom from thiophene, and what remains of the ring structure cross-links with another equivalent to form one-half equivalent of cyclooctatetraene. A similar reaction may occur with the polymeric rr-P3HT system; cross-linking may occur between neighboring polymer chains following sulfur abstraction from each. The use of DFT calculations to determine the relative energetic stability of $(CaS)_n$ clusters ($n = 1 - \infty$) showed that the enthalpy of this proposed reaction was similar to that measured calorimetrically for $n = 3$ to 4. Importantly, there seems to be no other reaction class that gives a heat of reaction (estimated using either tabulated heats or DFT) anywhere near as large.

Ca gas atoms that strike the rr-P3HT surface enter a weakly held, mobile adsorbed state from which they either (*a*) desorb, (*b*) diffuse under the surface and react with available thiophene sulfur atoms, or (*c*) diffuse across the surface to find other Ca atoms and make Ca-Ca bonds, thereby forming Ca clusters and eventually a continuous Ca film on the polymer. The atoms that desorb do not contribute to the measured heat of adsorption, so we do not discuss them further. For coverages from 0 to 0.5 ML, Ca atoms react predominantly with thiophene sulfur atoms below the polymer surface, which is consistent with the measured reaction energetics and the proposed reaction scheme. Once the sulfur atoms in the first layer of the polymer surface react with Ca, kinetic competition occurs between the adsorbing Ca atoms (*a*) migrating to and permanently adsorbing to Ca islands on the surface and (*b*) diffusing under the surface to find thiophene groups with which to react. In this coverage range, the measured enthalpy of adsorption per mole of adsorbing Ca (ΔH_{meas}) is related to both the energetics of each process ($\Delta H_a \cong$ 178 kJ mol^{-1}, $\Delta H_b \cong$ 405 kJ mol^{-1}) and the percentage of adsorbing Ca atoms undergoing each process [$\Delta H_{meas} = \%a(\Delta H_a) + \%b(\Delta H_b)$]. As the coverage increases, so does the depth of subsurface diffusion necessary for Ca to find an unreacted thiophene ring, rendering this process less kinetically favored over the formation of three-dimensional Ca islands. ΔH_{meas} subsequently

HAP: hydroxyapatite

decreases from the initial value (corresponding to $\%b = 100$) to the heat measured for $\%a = 100$ (~5 ML Ca coverage), in which all adsorbing Ca atoms adsorb to Ca islands, eventually forming multilayer Ca.

These findings show that the adsorption of Ca to the P3HT surface, using methods similar to those used in device preparation, results in the destruction of the original molecular (and therefore electronic) structure of the polymer at the interface between the two materials. This transformation of the polymer structure could negatively affect device performance. However, one can suppress this aggressive subsurface reaction by cooling the substrate to subambient temperatures during metal atom deposition (47). It is hoped that these fundamental studies will lead to improved procedures for the preparation of these important electrode-polymer interfaces and, eventually, to organic electronic devices with improved performance.

6. INVESTIGATIONS OF PROTEIN ADSORPTION WITH ISOTHERMAL TITRATION CALORIMETRY

ITC has been successfully utilized for adsorption calorimetry measurements, as demonstrated by Goobes et al. (48, 49) in their investigations of biologically relevant protein-mineral interactions. These authors used a commercially available ITC system, the MicroCal iTC$_{200}$™ (GE Healthcare, Uppsala, Sweden), that was first described in 1989 by Wiseman et al. (50). This system comprises sample and reference cells, a sample-delivery apparatus, and a system for measuring the power consumption required to maintain isothermal sample and reference cell conditions.

Goobes et al. (48) used ITC along with equilibrium adsorption isotherm analysis to study the adsorption of statherin onto hydroxyapatite (HAP) crystals. Statherin is a 5,380-Da salivary protein that is important to the electrolyte balance necessary for maintaining tooth enamel. The ionic components of HAP are supersaturated in the oral cavity, but the nucleation and growth of the mineral are inhibited by the presence of statherin. In an initial study, adsorption measurements were used to examine the driving forces and mechanisms involved in statherin adsorption onto the HAP surface (48). Another study investigated the role of statherin's N-terminal primary sequence in protein-surface binding (49). What made these studies exceptionally powerful was that Goobes et al., in collaboration with the Drobny group (51–55), also characterized the structure of the adsorbed protein; therefore, these studies were the first to apply adsorption calorimetry to the study of the energy of a protein's absorption, for which the protein's structure had also been experimentally characterized.

An example of the ITC results is shown in **Figure 6**, in which the measured heat of reaction is plotted versus the molar ratio C_t/M_t', in which C_t is the total concentration of injected statherin and M_t' is the maximal concentration of statherin-binding sites on the crystal surface. Using calorimetric measurements at temperatures between 15°C and 37°C, and the relationship $\Delta G° = RT \ln K = \Delta H - T\Delta S°$, the authors determined the equilibrium association constant (K), the enthalpy change of adsorption (ΔH), the fraction of binding sites with the measured adsorption enthalpy, the Gibbs free-energy change ($\Delta G°$), and the standard entropy change ($\Delta S°$). Statherin binds to two types of sites on HAP, described as sites **A** and **B**. **A** sites, which are occupied first, are characterized by a measurable, exothermic heat of adsorption and make up ~11–21% of the total protein-binding mineral-surface sites. **B** sites, which make up the rest of the surface and are populated after the **A** sites are saturated, do not display a measurable heat of adsorption. For both binding interactions, the favorable free energy of adsorption is dominated by a very large positive change in entropy, which probably arises from the release of organized water from both the protein and HAP surfaces. In addition, data taken with different buffer environments indicate that proton transfer plays a role in this protein-mineral interaction. From a biological standpoint, these results

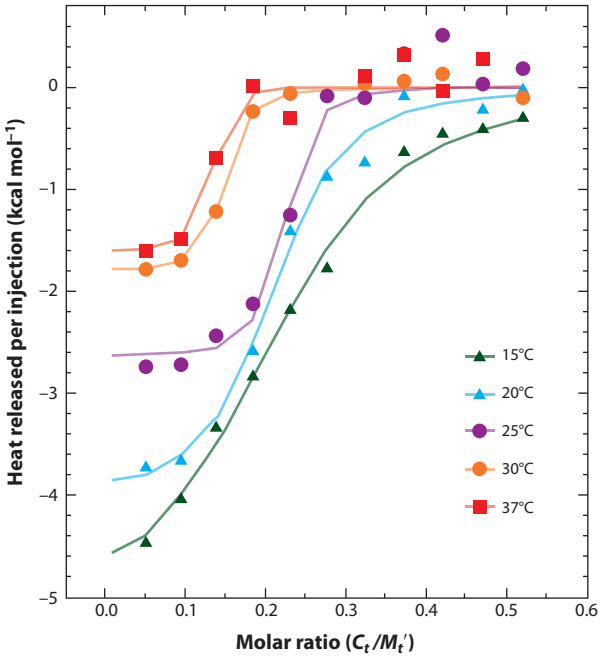

Figure 6

Isothermal titration calorimetry data, corrected for the heat of dilution, obtained at different temperatures for statherin adsorbing onto crystals of hydroxyapatite (HAP) suspended in buffer. The heat of reaction is plotted as a function of HAP surface coverage, which is expressed as the ratio of the total injected statherin (C_t) to the maximal concentration of statherin-binding sites (M_t'). Reprinted with permission from Reference 48. Copyright 2006, American Chemical Society.

are interesting because a low adsorption enthalpy and the occurrence of proton transfer suggest that adsorption reversibility and pH dependency allow the statherin-HAP system to dynamically respond to biologically important variations in the salivary environment. Remarkably, the heats of adsorption are small in this case compared with the much larger heats of adsorption for much smaller organic molecules onto clean Pt surfaces (1, 10).

In Goobes et al.'s (49) second study, the authors evaluated the role of the basic amino acids near the protein's N terminus using ITC, equilibrium adsorption isotherm analysis, and solid-state NMR (49). The acidic residues at the N terminus are well characterized and interact strongly with the surface of HAP, but the role of the nearby basic residues is less well understood. Mutants of wild-type statherin were generated with single and multiple point mutations of the basic residues (replacement with alanine) near the N terminus, and the thermodynamics of wild-type and mutant statherin adsorption were probed through equilibrium adsorption isotherm analysis and ITC.

Single point mutations did not have a significant effect on the equilibrium association constant, packing density, or initial adsorption enthalpy. However, simultaneous mutation of all four of the basic amino acids significantly reduced both the equilibrium association constant (by a factor of five) and the maximum surface coverage of the protein (to 50% of the wild type), although the initial adsorption enthalpy remained approximately the same. Further studies are required to completely describe the structural changes that underlie these thermodynamics, but the results clearly show that specific amino acid residues—even those not directly involved in protein-protein or protein-surface binding—can have significant effects on these interactions and, potentially, on

any associated biological processes. The lack of measurable changes upon single site mutations also demonstrates the functional robustness of this biological system as well as the ability of proteins to function as intended, even with primary sequence alterations.

7. ELECTROCHEMICAL ADSORPTION CALORIMETRY

An exciting recent development demonstrates that the measurement of surface-temperature changes resulting from adsorption events can also be used to obtain valuable information about electrochemical reactions at flat electrode surfaces. Schuster's group (3–5) has developed a novel electrochemical microcalorimetry instrument that employs a PVDF pyroelectric heat detector; the design of this instrument is similar to that of the SCAC detector created by the Campbell group (12, 16, 56). Schuster and colleagues redesigned the detector to measure temperature changes to the working electrode so as to obtain information about the thermodynamics of electrochemical reactions.

The redesigned instrument consists of a 9-μm-thick PVDF heat detector foil (coated on the front and back faces with aluminum) pressed against the back face of a working electrode (3–5). The suction method the authors used to apply pressure at this PVDF-electrode contact was very effective. To minimize pyroelectric and piezoelectric noise, and to allow experiments to be conducted under an inert atmosphere, the entire instrument was contained in an airtight, thermally insulating container. Heat evolved from an electrochemical reaction provides information about the entropy of reversible reactions, as well as about reaction pathways and irreversible processes. This electrochemical microcalorimeter allows heats of reactions corresponding to a few percent of an ML of surface coverage to be measured, thereby providing fundamental information about electrochemical reactions that is inaccessible through other techniques.

Future goals for electrochemical calorimetry include the use of single-crystal electrodes, which will greatly improve our fundamental understanding of how reaction energetics correlate with specific reaction pathways, surface structures, and crystal faces. In addition, planned efforts to increase sensitivity and lower detection limits will allow the investigation of processes with lower Peltier heats, such as surface ordering and phase transitions.

8. FUTURE DIRECTIONS: HIGH-THROUGHPUT, ARRAY-BASED ADSORPTION MICROCALORIMETRY

The results described above demonstrate pyroelectric heat-detection methods for adsorption microcalorimetry that are well suited to applications in microarray-based devices for high-throughput adsorption calorimetry. High-throughput adsorption calorimetry is envisioned to be very useful for the screening of materials and fundamental studies in surface chemistry, as detailed below.

Figure 7 depicts an array detector that would utilize independent, addressable electrodes mounted on one side of a pyroelectric material, such as a thin sheet of PVDF for studies below 350 K or lithium niobate or lithium tantalate for studies up to ~1,000 K (57). The other side of the pyroelectric material would be completely coated with a continuous electrode (an Au film, for example), which would be locally coated or functionalized differently above each different addressable electrode. This setup would allow the adsorption of an analyte to many different surface coatings to be screened simultaneously in a single, high-throughput experiment. The use of a nearby electrode as a reference signal (to subtract unwanted signal due to temperature drift or injection of a new fluid above the array) would greatly improve detection limits, such that it could even be used to probe adsorption heats from liquid solutions in addition to gases.

Such an instrument would be very useful for the high-throughput screening of materials. In many technologies, it would be useful to screen materials with respect to the strength of their

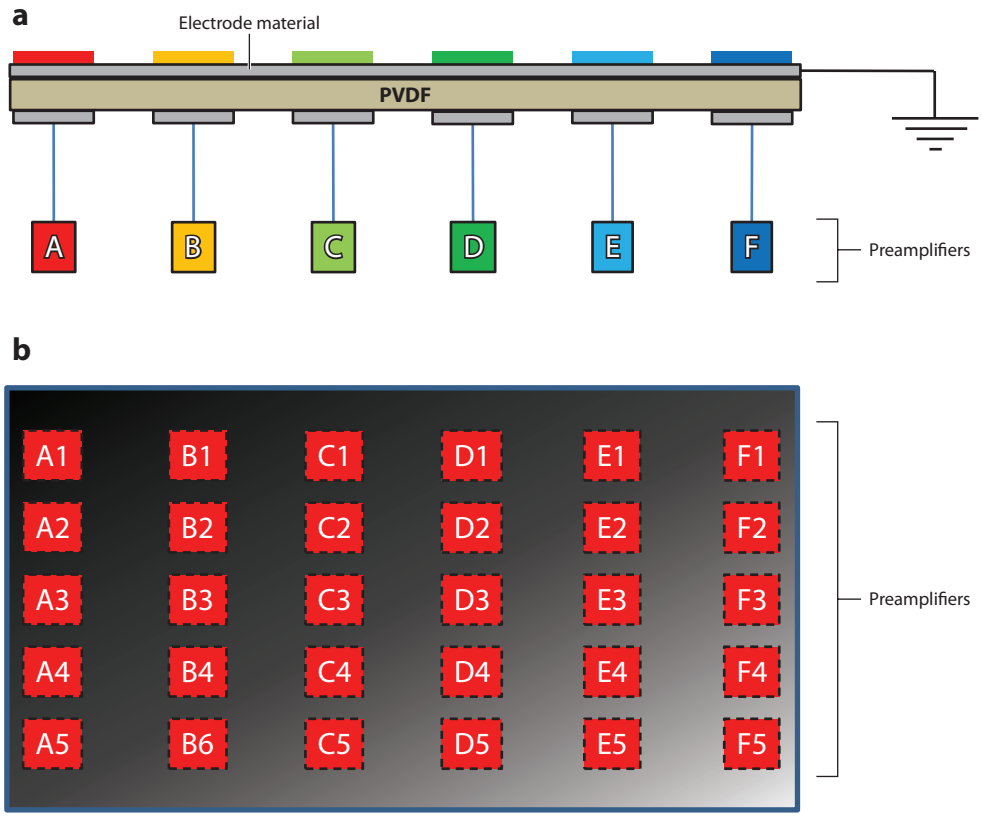

Figure 7

Schematics of proposed (*a*) one- and (*b*) two-dimensional adsorption microcalorimeter detector microarrays based on pyroelectric polyvinylidene fluoride (PVDF) with separately addressable microelectrodes on the bottom. The regions above such microelectrodes would be functionalized or coated with different species or materials (*indicated with different colors*). Electrode material is shown in gray; the colored, lettered boxes represent preamplifiers, with colors representing the specific regions of surface functionalization at which reaction thermodynamics are being measured.

interactions with molecules in the gas phase or in liquid solutions. For example, learning how the functionalization of surfaces with different organic functionalities or polymer films influences the strength of adsorption could lead to the development of better chemical or biochemical sensors. This instrument design could also provide a high-throughput approach to improving our fundamental understanding of molecule-surface interactions and even protein-solid or protein-ligand binding. Because the top electrode could be made of Au, such studies could be performed together with surface plasmon resonance microscopy to simultaneously determine the amount of adsorbate produced at each element of the array. Methods for high-throughput quantitative analysis of adsorption amounts from liquid solutions, with 1-s time resolution and sensitivity to ~0.1% ML adsorbed protein, that in principle could be coupled with array-based adsorption microcalorimetry, have been recently reviewed (58).

Array-based calorimetry could also be used for catalyst screening. When the catalytic reaction being studied is exothermic or endothermic, it respectively heats or cools the catalyst surface. The faster the reaction that occurs on a particular element of the array (i.e., the better the catalyst material there), the more heating or cooling occurs. This temperature change could easily be detected

and certainly should be more sensitive than the infrared radiation "thermography" detectors that are currently in use (59–61). A surface gradient of several transition-metal concentrations could be prepared through multiple-nozzle vapor deposition, for example, and many catalyst candidates could be screened in a single experiment.

In the future, techniques such as SCAC, ITC, and electrochemical calorimetry will continue to provide data crucial to research and development in many areas of science and technology. We hope that continued research in this area will result in exciting new instrumentation that will increase both the power and the routine applicability of adsorption calorimetry.

DISCLOSURE STATEMENT

The authors are not aware of any affiliations, memberships, funding, or financial holdings that might be perceived as affecting the objectivity of this review.

ACKNOWLEDGMENTS

The authors' work was supported by the National Science Foundation (CHE-0757221) and by the U.S. Department of Energy, Office of Basic Energy Sciences, Chemical Sciences Division (DE-FG02-96ER14630). The authors thank the past and present members of the Campbell research group and the departmental support staff for their hard work and commitment to excellence.

LITERATURE CITED

1. Campbell CT, Lytken O. 2009. Experimental measurements of the energetics of surface reactions. *Surf. Sci.* 603:1365–72
2. Blandamer MJ, Cullis PM, Engberts JBFN. 1998. Titration microcalorimetry. *J. Chem. Soc. Faraday Trans.* 94:2261–67
3. Etzel KD, Bickel KR, Schuster R. 2010. A microcalorimeter for measuring heat effects of electrochemical reactions with submonolayer conversions. *Rev. Sci. Instrum.* 81:034101
4. Etzel KD, Bickel KR, Schuster R. 2010. Heat effects upon electrochemical copper deposition on polycrystalline gold. *ChemPhysChem* 11:1416–24
5. Schuster R, Rösch R, Timm AE. 2007. Microcalorimetry of electrochemical reactions at submonolayer conversions. *Z. Phys. Chem.* 221:1479–91
6. Borroni-Bird CE, Al-Sarraf N, Andersson S, King DA. 1991. Single-crystal adsorption microcalorimetry. *Chem. Phys. Lett.* 183:516–20
7. Borroni-Bird CE, King DA. 1991. An ultrahigh vacuum single crystal adsorption microcalorimeter. *Rev. Sci. Instrum.* 62:2177–85
8. Stuckless JT, Al-Sarraf N, Wartnaby C, King DA. 1993. Calorimetric heats of adsorption for CO on nickel single crystal surfaces. *J. Chem. Phys.* 99:2202–12
9. Dixon-Warren SJ, Kovar M, Wartnaby CE, King DA. 1994. Pyroelectric single crystal adsorption microcalorimetry at low temperatures: oxygen on Ni(100). *Surf. Sci.* 307:16–22
10. Brown WA, Kose R, King DA. 1998. Femtomole adsorption calorimetry on single-crystal surfaces. *Chem. Rev.* 98:797–831
11. Stuckless JT, Starr DE, Bald DJ, Campbell CT. 1997. Metal adsorption calorimetry and adhesion energies on clean single-crystal surfaces. *J. Chem. Phys.* 107:5547–53
12. Stuckless JT, Frei NA, Campbell CT. 1998. A novel single-crystal adsorption calorimeter and additions for determining metal adsorption and adhesion energies. *Rev. Sci. Instrum.* 69:2427–38
13. Stuckless JT, Frei NA, Campbell CT. 2000. Pyroelectric detector for single-crystal adsorption microcalorimetry: analysis of pulse shape and intensity. *Sens. Actuators B* 62:13–22
14. Starr DE, Campbell CT. 2001. Low-temperature adsorption microcalorimetry: Pb on MgO(100). *J. Phys. Chem. B* 105:3776–82

15. Diaz SF, Zhu JF, Shamir N, Campbell CT. 2005. Pyroelectric heat detector for measuring adsorption energies on thicker single crystals. *Sens. Actuators B* 107:454–60
16. Lew W, Lytken O, Farmer JA, Crowe MC, Campbell CT. 2010. Improved pyroelectric detectors for single crystal adsorption calorimetry from 100 to 350 K. *Rev. Sci. Instrum.* 81:024102
17. Lang SB. 2005. Pyroelectricity: from ancient curiosity to modern imaging tool. *Phys. Today* 58:31–36
18. Beeck O, Cole WA, Wheeler A. 1950. Determination of heats of adsorption using metal films. *Discuss. Faraday Soc.* 8:314–21
19. Lytken O, Lew W, Harris JJW, Vestergaard EK, Gottfried JM, Campbell CT. 2008. Energetics of cyclohexene adsorption and reaction on Pt(111) by low-temperature microcalorimetry. *J. Am. Chem. Soc.* 130:10247–57
20. Ibos L, Teyssedre G, Bernes A, Lacabanne C. 1999. Thermal ageing of pyroelectricity in PVDF and P(VDF-TrFE) copolymers. *SPIE* 4017:29–36
21. Punckt C, Bodega PS, Rotermund HH. 2006. Quantitative measurement of the deformation of ultra-thin platinum foils during adsorption and reaction of CO and O_2. *Surf. Sci.* 600:3101–9
22. Lytken O, Lew W, Campbell CT. 2008. Catalytic reaction energetics by single crystal adsorption calorimetry: hydrocarbons on Pt(111). *Chem. Soc. Rev.* 37:2172–79
23. Ranney JT, Starr DE, Musgrove JE, Bald DJ, Campbell CT. 1999. A microcalorimetric study of the heat of adsorption of copper on well-defined oxide thin film surfaces: MgO(100), p(2 × 1) Mo oxide on Mo(100) and disordered W oxide. *Faraday Discuss.* 114:195–208
24. Campbell CT, Starr DE. 2002. Metal adsorption and adhesion energies on MgO(100). *J. Am. Chem. Soc.* 124:9212–18
25. Campbell CT, Peden CHF. 2005. Chemistry: oxygen vacancies and catalysis on ceria surfaces. *Science* 309:713–14
26. Xu L, Henkelman G, Campbell CT, Jonsson H. 2005. Small Pd clusters, up to the tetramer at least, are highly mobile on the MgO(100) surface. *Phys. Rev. Lett.* 95:1461031
27. Xu L, Henkelman G, Campbell CT, Jonsson H. 2006. Pd diffusion on MgO(100): the role of defects and small cluster mobility. *Surf. Sci.* 600:1351–62
28. Zhu J, Farmer JA, Ruzycki N, Xu L, Campbell CT, Henkelman G. 2008. Calcium adsorption on MgO(100): energetics, structure, and role of defects. *J. Am. Chem. Soc.* 130:2314–22
29. Farmer JA, Campbell CT, Xu L, Henkelman G. 2009. Defect sites and their distributions on MgO(100) by Li and Ca adsorption calorimetry. *J. Am. Chem. Soc.* 131:3098–103
30. Farmer JA, Ruzycki N, Zhu JF, Campbell CT. 2009. Lithium adsorption on MgO(100) and its defects: charge transfer, structure, and energetics. *Phys. Rev. B* 80:0354181
31. Farmer JA, Baricuatro JH, Campbell CT. 2010. Ag adsorption on reduced CeO_2(111) thin films. *J. Phys. Chem. C* 114:17166–72
32. Campbell CT, Parker SC, Starr DE. 2002. The effect of size-dependent nanoparticle energetics on catalyst sintering. *Science* 298:811–14
33. Parker SC, Campbell CT. 2007. Kinetic model for sintering of supported metal particles with improved size-dependent energetics and applications to Au on TiO_2(110). *Phys. Rev. B: Condens. Matter Mater. Phys.* 75:0354301
34. Farmer JA, Campbell CT. 2010. Ceria maintains smaller metal catalyst particles by strong metal-support binding. *Science* 329:933–36
35. Schwartz JM, Schmidt LD. 1992. Microstructures of Pt-Ce and Rh-Ce particles on alumina and silica. *J. Catal.* 138:283–93
36. Kalakkad D, Datye AK, Robota H. 1992. Interaction of platinum and ceria probed by transmission electron microscopy and catalytic reactivity. *Appl. Catal. B: Environ.* 1:191–219
37. Kundakovic L, Flytzani-Stephanopoulos M. 1998. Cu- and Ag-modified cerium oxide catalysts for methane oxidation. *J. Catal.* 179:203–21
38. Fischer-Wolfarth J-H, Farmer JA, Flores-Camacho JM, Genest A, Yudanov IV, et al. 2010. Particle-size dependent heats of adsorption of CO on supported Pd nanoparticles as measured with a single-crystal microcalorimeter. *Phys. Rev. B* 81:241416

39. Schalow T, Brandt B, Starr DE, Laurin M, Shaikhutdinov SK, et al. 2007. Particle size dependent adsorption and reaction kinetics on reduced and partially oxidized Pd nanoparticles. *Phys. Chem. Chem. Phys.* 9:1347–61
40. Zhu J, Bebensee F, Hieringer W, Zhao W, Baricuatro JH, et al. 2009. Formation of the calcium/poly(3-hexylthiophene) interface: structure and energetics. *J. Am. Chem. Soc.* 131:13498–507
41. Bebensee F, Zhu J, Baricuatro JH, Farmer JA, Bai Y, et al. 2010. Interface formation between calcium and electron-irradiated poly(3-hexylthiophene). *Langmuir* 26:9632–39
42. Reese MO, White MS, Rumbles G, Ginley DS, Shaheen SE. 2008. Optimal negative electrodes for poly(3-hexylthiophene): [6,6]-phenyl C61-butyric acid methyl ester bulk heterojunction photovoltaic devices. *Appl. Phys. Lett.* 92:053307
43. Reese MO, Morfa AJ, White MS, Kopidakis N, Shaheen SE, et al. 2008. Pathways for the degradation of organic photovoltaic P3HT:PCBM-based devices. *Sol. Energy Mater. Sol. C.* 92:746–52
44. Paci B, Generosi A, Albertini VR, Perfetti P, de Bettignies R, Sentein C. 2008. Time-resolved morphological study of organic thin film solar cells based on calcium/aluminum cathode material. *Chem. Phys. Lett.* 461:77–81
45. Hsieh S-N, Kuo T-Y, Chong L-W, Wen T-C, Yang F-S, et al. 2009. A study of semitransparent cathodes on the performance of top-emitting polymer light-emitting diodes. *IEEE Photonic Tech. Lett.* 21:109–11
46. Bröms P, Birgersson J, Johansson N, Lögdlund M, Salaneck WR. 1995. Calcium electrodes in polymer LEDS. *Synth. Met.* 74:179–81
47. Bebensee F, Schmid M, Steinrück H-P, Campbell CT, Gottfried JM. 2010. Towards well-defined metal-polymer interfaces: temperature-controlled suppression of subsurface diffusion and reaction at the Ca/P3HT interface. *J. Am. Chem. Soc.* 132:12163–65
48. Goobes R, Goobes G, Campbell CT, Stayton PS. 2006. Thermodynamics of statherin adsorption onto hydroxyapatite. *Biochemistry* 45:5576–86
49. Goobes R, Goobes G, Shaw WJ, Drobny GP, Campbell CT, Stayton PS. 2007. Thermodynamic roles of basic amino acids in statherin recognition of hydroxyapatite. *Biochemistry* 46:4725–33
50. Wiseman T, Williston S, Brandts JF, Lin L-N. 1989. Rapid measurement of binding constants and heats of binding using a new titration calorimeter. *Anal. Biochem.* 179:131–37
51. Long JR, Dindot JL, Zebroski H, Kiihne S, Clark RH, et al. 1998. A peptide that inhibits hydroxyapatite growth is in an extended conformation on the crystal surface. *Proc. Natl. Acad. Sci. USA* 95:12083–87
52. Shaw WJ, Long JR, Dindot JL, Campbell AA, Stayton PS, Drobny GP. 2000. Determination of statherin N-terminal peptide conformation on hydroxyapatite crystals. *J. Am. Chem. Soc.* 122:1709–16
53. Shaw WJ, Long JR, Campbell AA, Stayton PS, Drobny GP. 2000. A solid state NMR study of dynamics in a hydrated salivary peptide adsorbed to hydroxyapatite. *J. Am. Chem. Soc.* 122:7118–19
54. Long JR, Shaw WJ, Stayton PS, Drobny GP. 2001. Structure and dynamics of hydrated statherin on hydroxyapatite as determined by solid-state NMR. *Biochemistry* 40:15451–55
55. Gibson JM, Raghunathan V, Popham JM, Stayton PS, Drobny GP. 2005. A REDOR NMR study of a phosphorylated statherin fragment bound to hydroxyapatite crystals. *J. Am. Chem. Soc.* 127:9350–51
56. Ajo HM, Ihm H, Moilanen DE, Campbell CT. 2004. Calorimeter for adsorption energies of larger molecules on single crystal surfaces. *Rev. Sci. Instrum.* 75:4471–80
57. Porter SG. 1981. A brief guide to pyroelectric detectors. *Ferroelectrics* 33:193–206
58. Campbell CT, Kim G. 2007. SPR microscopy and its applications to high-throughput analyses of biomolecular binding events and their kinetics. *Biomaterials* 28:2380–92
59. Hagemeyer A, Jandeleit B, Liu Y, Poojary DM, Turner HW, et al. 2001. Applications of combinatorial methods in catalysis. *Appl. Catal.* 221:23–43
60. McFarland EW, Archibald WB. 2003. Infrared spectroscopic imaging of libraries. *U.S. Patent No. 6,541,271*
61. Archibald WB, Hornbostel M. 2003. Parallel screen for rapid thermal characterization of materials. *U.S. Patent No. 6,536,944*
62. Sai N, Li ZQ, Martin MC, Basov DN, Di Ventra M. 2007. Electronic excitations and metal-insulator transition in poly(3-hexylthiophene) organic field-effect transistors. *Phys. Rev. B* 75:0453071
63. Diaz SF, Zhu JF, Harris JJW, Goetsch P, Merte LR, Campbell CT. 2005. Heats of adsorption of Pb on pristine and electron-irradiated poly(methyl methacrylate) by microcalorimetry. *Surf. Sci.* 598:22–34

Annual Review of
Analytical Chemistry

Volume 4, 2011

Contents

Indexes

Errata

An online log of corrections to the *Annual Review of Analytical Chemistry* articles may be found at http://arjournals.annualreviews.org/errata/anchem